

Kennesaw State University
DigitalCommons@Kennesaw State University

Master of Science in Integrative Biology Theses

Department of Ecology, Evolution, and Organismal
Biology

Spring 5-14-2019

The Role of Reactive Oxygen Species in *Crotalus atrox* Venom-induced Cell Death

Lindsay Brown

Follow this and additional works at: https://digitalcommons.kennesaw.edu/integrbiol_etd

Part of the [Integrative Biology Commons](#)

Recommended Citation

Brown, Lindsay, "The Role of Reactive Oxygen Species in *Crotalus atrox* Venom-induced Cell Death" (2019). *Master of Science in Integrative Biology Theses*. 38.

https://digitalcommons.kennesaw.edu/integrbiol_etd/38

This Thesis is brought to you for free and open access by the Department of Ecology, Evolution, and Organismal Biology at DigitalCommons@Kennesaw State University. It has been accepted for inclusion in Master of Science in Integrative Biology Theses by an authorized administrator of DigitalCommons@Kennesaw State University. For more information, please contact digitalcommons@kennesaw.edu.

**The Role of Reactive Oxygen Species in *Crotalus atrox* Venom-
induced Cell Death**

By Lindsay Brown

**A Thesis Presented in Partial Fulfillment of Requirements for the Master of Science in
Integrative Biology for the Department of Molecular and Cellular Biology**

**Kennesaw State University
1000 Chastain Road Kennesaw,
GA 30144 May 2015**

Dr. Eric A. Albrecht, Thesis Advisor

Associate Professor of Biology
Department of Molecular and Cellular Biology
Kennesaw State University

Dr. Carol Chrestensen

Professor of Chemistry
Department of Chemistry and Biochemistry
Kennesaw State University

Dr. Thomas McElroy

Associate Professor of Biology
Department of Ecology, Evolution, and Organismal Biology
Kennesaw State University

Abstract

Venomous snake bites impact humans all around the world. Anti-venom treatments mitigate systemic effects such as vascular hemorrhage, platelet aggregation inhibition, and the activation of inflammatory mediators. However, hemorrhagic snake venom also causes a loss of cellular adhesion to extracellular matrix components resulting in massive local tissue damage. To better understand the mechanism in which venom induces local tissue damage, human embryonic kidney cells (HEKS) were grown on PEI then stimulated with 500 μ g/ml *Crotalus atrox* (CA) venom for 4 and 10 hours. Alamar Blue assays were used to measure cell viability and results suggest a 15 \pm 8.6% ($p < 0.05$) and 59 \pm 10.7% ($p < 0.05$) reduction in cell viability at 4 and 10 hours, respectively. Cells stimulated with 500 μ g/ml venom for 10 hours stained 98 \pm 2.2% ($p < 0.05$) positive for Trypan blue, suggesting the venom reduces membrane integrity. Identical treatment in the presence of 200 units PEG-catalase (PC) increased viability by 37 \pm 5.7% ($p > 0.001$) compared to cells stimulated with venom alone. 2',7'-Dichlorofluorescein-diacetate (DCF-DA) was used to quantify reactive oxygen species during venom stimulation. HEK cells stimulated with 50 μ g/ml *Crotalus atrox* resulted in a 336-fold increase in ROS-induced fluorescence between 1 and 2 hours ($p < 0.001$). Pre-treating the cells with 200 Units peg-catalase for 2 hours before venom stimulation resulted in 425-fold decrease in ROS-induced fluorescence that persisted over the 4 hour stimulation period ($p < 0.0001$). Peg-catalase resulted in a greater decrease in fluorescence over time than other treatments including N-acetyl cysteine (NAC), SOD1 inhibitor LCS-1, and NOX inhibitor VAS2870. This suggests hydrogen peroxide is

produced during venom induced injury and plays a critical role in venom mediated cell death.

Table of Contents

Abstract.....	2
Table of Contents.....	4
Introduction.....	5
Materials and Methods.....	10
Results.....	13
Discussion.....	25
Conclusion.....	33
Future Directions.....	34
Integration of Thesis Research.....	34
Acknowledgements.....	35
References.....	36

Introduction

Components of Hemorrhagic Snake Venom

There are approximately 100,000 snakebite-associated fatalities every year (1). Systemic effects of many venomous snakebites include vascular hemorrhage, platelet aggregation inhibition, and activation of inflammatory mediators, while local symptoms consist of tissue edema and necrosis. For example, bites from *Crotalus atrox* (western diamond back rattlesnake) cause tissue destruction by cleaving proteins, such as collagen, inhibiting cellular attachment to the basement membrane, a protein rich cell-adherent matrix (2-4). This toxic activity is due to bioactive proteins such as snake venom metalloproteinases (SVMPs), L-amino acid oxidases (LAAOs) and disintegrins present in the venom. SVMPs make up approximately 30% of the total protein present in hemorrhagic venom and require zinc cofactors to cleave type IV collagen present in the basement membrane (5-7). For instance, Ht-d, a hemorrhagic toxin, is an SVMP from *C. atrox* venom that disrupts capillaries by enzymatically cleaving type IV collagen. Although the mechanism of Ht-d is thought to be similar to that of collagenases, the exact mechanism is unknown (8). Actions of SVMPs are responsible for hemorrhage and pro-inflammatory responses seen during hemorrhagic snake venom associated injuries (7).

L-amino acid oxidases (LAAOs) are flavoenzymes that oxidatively deaminate L-amino acids. The by-products of this enzymatic reaction include ammonia and hydrogen peroxide. Many reports show that the effects of LAAOs may be due to the generation of hydrogen peroxide, which then acts directly on membranes, proteins, and DNA (9,10). Apoxin I, a protein found in *Crotalus atrox* venom, has been reported to have LAAO

activity. This toxin mediated apoptosis in part through hydrogen peroxide production, which is inhibited by catalase, a hydrogen peroxide scavenging enzyme found within the cells (11).

In contrast to the proteolytic destruction of tissue by enzymatic activity, disintegrins are small, non-enzymatic cysteine-rich proteins with Arg-Gly-Asp (RGD) sequences that selectively bind to integrins present on platelets and endothelial cells, inhibiting platelet aggregation and attachment to the extracellular matrix (ECM) (12). For example, crostatroxin 2, a disintegrin found specifically in *Crotalus atrox* venom, inhibits platelet aggregation induced by ADP by blocking the binding of fibrinogen to $\alpha 5\beta 1$ integrin found on the platelet surface. Other disintegrins such as eristostatin inhibit the $\alpha 4\beta 1$ integrin (13). Collectively, disruption of tissue connections in adherent cell types by SVMPs, LAAOs, and disintegrins can lead to a specific type of apoptosis termed anoikis (14).

Cell Death by Cellular Detachment: Anoikis

The first objective of this study was to determine the effects of *Crotalus atrox* venom on viability and adherence. We hypothesized that enhancing cellular attachment would improve viability of *C. atrox* venom stimulated HEK-293T cells. To do this, collagen and polyethylenimine (PEI) were used to test two different methods to enhance cellular attachment. Collagen, a protein naturally present in the extracellular matrix, aids in cellular attachment by increasing protein-protein interaction between the cells and the culture dish. PEI, a poly-cation, attaches to the culture dish and its positive charge increases the electrostatic interaction with the negatively charged glycocalyx, a layer of glycolipids and glycoproteins that cover the cellular membrane. Because hemorrhagic

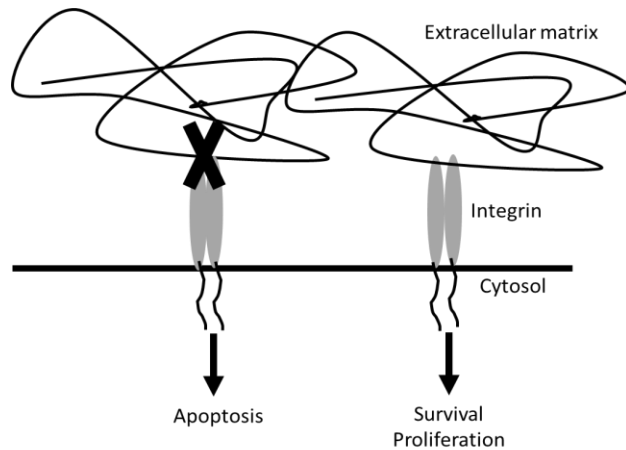


Figure 1. Integrin mediated attachment to components of ECM activates survival signaling while loss of attachment activates apoptosis.

snake venom disrupts tissues, it may promote anoikis. Anoikis is a specific type of apoptosis that occurs when the attachment of cells to the extracellular matrix (ECM) is disrupted or lost. Under normal conditions, integrins bound to ECM proteins elicit survival signals that suppress the activation of the intrinsic apoptotic pathways. When cells are adhered to the ECM via integrins,

phosphatidylinositol-3-kinase (PI3K)-mediated AKT activity stimulates leukemia-2 (Bcl-2) expression promoting cell survival and proliferation (13-15). (**Figure 1**). However, the action of disintegrins and SVMs among other bioactive molecules found in venom can lead to loss of cellular attachment resulting in disrupted integrin-mediated survival signals. Loss of integrin-ECM interaction causes an activation of pro-apoptotic (intrinsic) pathways. Intrinsic apoptotic signaling pathways include a series of complex events involving mitochondrial disruption and are responsible for mediating anoikis (13-15). In this pathway, initiation of Bax (Bcl-2-associated X protein) and Bak (Bcl-2 homologous antagonist killer) create a channel in the outer membrane of the mitochondria allowing for the release of cytochrome c into the cytosol. Cytochrome c then interacts caspase-9 and Apaf (apoptosis protease activating factor) forming what is known as the apoptosome, a complex that activates caspase-9. Caspase-9 is an initiator caspase that activates execution caspases-3, -6, and -7 (16). Caspase-3

inactivates ICAD, the inhibitor of caspase activated DNase (CAD). Once ICAD is inactivated, CAD can dimerize and cause double stranded breaks in DNA causing severe DNA fragmentation and subsequent cell death (16).

Mitochondrial Disruption and ROS Generation

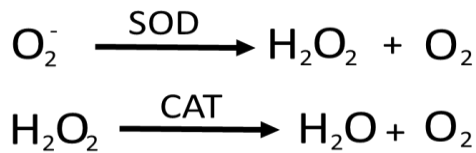


Figure 2. Diagram of Superoxide and Hydrogen Peroxide Conversion.

Superoxide is converted to hydrogen peroxide by superoxide dismutase (SOD). Hydrogen peroxide is converted to water and molecular oxygen by catalase (CAT).

Our next objective was to determine if intracellular ROS are generated during venom stimulation and if they play an important role in the mechanism of venom induced cell death. We hypothesized that reducing ROS during venom stimulation would be cytoprotective. PEG-catalase and N-acetyl cysteine were used as two

separate methods to reduce intracellular ROS. Polyethylene glycol (PEG) is attached to catalase to allow for increased permeability. Dichlorofluorescein-diacetate, a ROS specific fluorescent probe, was used to measure ROS levels in venom stimulated HEK-293T. Mitochondrial injury resulting from pro-apoptotic signaling cascades generate excessive reactive oxygen species (ROS) such as superoxide, hydrogen peroxide, and hydroxyl ion, among others (17-20). Superoxide and hydroxyl ions are considered radical forms of ROS because they have unpaired electrons while hydrogen peroxide is a non-radical ROS. Radical forms are more reactive than non-radical forms because they can combine their unpaired electrons with that of another radical or they can donate or receive an electron from another molecule (21-22). This makes superoxide highly reactive and short-lived compared to hydrogen peroxide. When superoxide is generated, it is spontaneously or enzymatically converted to hydrogen peroxide by

superoxide dismutase. Catalase, an enzyme found with the peroxisome of our cells, converts hydrogen peroxide to water and molecular oxygen (**Figure 2**).

Hydrogen peroxide is produced in cells via a number of mechanisms including being a byproduct of cellular respiration. As such, it is highly abundant in aerobic organisms. Although it can be converted spontaneously or enzymatically to other more reactive ROS such as the hydroxyl radical, it is relatively stable. While high concentrations of hydrogen peroxide can be toxic, it is also an important signaling molecule reported to play a role in cell development, proliferation, and cell death (17-21, 23). For cells to function properly, a balance between production and consumption of ROS must be maintained. Many mechanisms exist by which cells maintain ROS homeostasis including the expression of enzymatic and non-enzymatic antioxidants. While superoxide dismutase and catalase enzymatically regulate levels of superoxide and hydrogen peroxide, glutathione is a potent non-enzymatic antioxidant that reacts with and neutralizes all ROS generated within cells (24). When these mechanisms fail due to cellular stress, ROS levels are elevated and the cell experiences increased oxidative stress. Oxidative stress can cause damage to lipids, DNA, organelles, protein structures, and altered expression of genes related to apoptosis cause cell death (23).

Phospholipids, the major component of biological membranes, are a main target of ROS due to the presence of highly reactive non-conjugated double bonds. ROS can remove a hydrogen atom from the double bond, which destabilizes the lipid with a radical that is open to react with molecular oxygen. As lipid peroxidation continues down the length of the fatty acid chain, oxidants are produced. As a part of objective two, we investigated membrane integrity after venom stimulation. Trypan blue, a dye

impermeable to cells unless the membrane has been compromised was used to determine if venom components target the plasma membrane.

It is reported that hemorrhagic venom induced injury elevates intracellular ROS (27-29). When exogenous stimuli, such as venom, induce oxidative stress, additional signaling pathways may be activated to control escalating ROS levels. For example, increased levels of ROS can lead to down regulation of cytochrome P450s and induction of anti-oxidant enzymes such as catalase and superoxide dismutase (27-31). This suggests that ROS could play a crucial role in the mechanism of venom-induced cell death. Therefore, the last objective of this study was to evaluate key oxidant producing enzymes, superoxide dismutase 1 (SOD1) and NADPH oxidase (NOX), for their contribution to ROS production during venom stimulation. Components of NADPH oxidase are assembled in the plasma membrane of cells when activated and produce superoxide and hydrogen peroxide as by-products. Superoxide dismutase 1 (SOD1) is found in the cytoplasm and converts superoxide to hydrogen peroxide. We hypothesized that inhibiting SOD1 and NOX would decrease ROS production and improve cell viability. LCS-1 (SOD1 inhibitor) and VAS2870 (NOX inhibitor) were used to show that SOD1 and NOX contribute to ROS production during venom stimulation. Thus, controlling reactive oxygen species may increase cell viability during venom-induced injury.

Materials and Methods

Cell Culture

Human embryonic kidney (HEK-293T) cells were cultured on tissue culture dishes in Dulbecco's Modified Eagle Medium (DMEM) containing 10% fetal calf serum

(FCS). Cells were grown in a humidified environment at 37°C buffered with 5% CO₂. Cells were passaged every 48-72 hours or until confluency was reached.

Cell Viability

Preparation of 96-well plates involved pre-treatment with 2.5µg/ml polyethylenimine (PEI) or 1% collagen for 30 minutes before adding 100µl of a 5x10⁵ cells/ml HEK suspension to each well. Cells were incubated for 24 hours at 37°C prior to experimentation. *Crotalus atrox* venom was purchased from Sigma, solubilized in phosphate buffered saline (PBS) and aliquots were stored at -80°C. Cells were treated with 10, 100, or 500µg/ml *Crotalus atrox* venom (CA) for 4 or 10 hours. For polyethylene glycol (PEG)-catalase (PC) and N-acetyl cysteine (NAC) viability experiments, cells were seeded on PEI or collagen treated 96-well plates as stated above. Cells were then pre-incubated with 200 units PEG-catalase for two hours or 3mM N-acetyl cysteine for 6 or 24 hours. Subsequently, cells were stimulated with 500µg/ml *Crotalus atrox* venom for 10 hours. For cytotoxicity experiments involving LCS-1 (SOD1 inhibitor) and VAS2870 (NOX inhibitor), cells were pre-incubated with 5, 7.5, or 10µM LCS-1 or 5, 7.5, or 10µM VAS2870 for 24 hours before stimulating with 500µg/ml *Crotalus atrox* venom for 10 hours. AlamarBlue Cell Viability reagent was used to measure viability according to manufacturer's protocol (32). The fluorescence intensity of AlamarBlue was measured using a Synergy H1 Hybrid Reader (Excitation 560nm, Emission 590nm). A minimum of two biological replicates were completed for each assay.

Phase contrast and brightfield microscopy

Phase contrast and brightfield imaging was used to evaluate cellular morphology during venom stimulation using an IX71 Olympus microscope coupled to Olympus

DP71 camera. Phase contrast micrographs (40X) and brightfield micrographs (10X) were taken of non-stimulated and venom stimulated cells after 4 or 10 hours for cytotoxicity experiments. For trypan blue studies and cytotoxicity experiments involving PEG-catalase and N-acetyl cysteine, bright field images were taken after 10 hours of venom stimulation.

Trypan Blue Membrane Integrity Assay

To examine membrane integrity, HEK-293T cells were suspended and diluted to a concentration of 5×10^5 cells/ml. Culture dishes (35mm) were treated with $2.5 \mu\text{g/ml}$ polyethylenimine (PEI) or 1% collagen before adding 1ml of cell suspension. Cells were incubated for 24 hours at 37°C . Cells were then treated with 10, 100, or $500 \mu\text{g/ml}$ *Crotalus atrox* venom for 10 hours. Media was removed and placed into a 1.5ml centrifuge tube and subsequently centrifuged for 1 minute. Cells were trypsinized, placed in corresponding centrifuge tube and centrifuged for 1 minute. Supernatant was removed and pellets were resuspended in 1ml of a 3:1 solution of PBS and 0.05% trypan blue. Cells were allowed to sit at room temperature for 5 minutes before counting with a hemocytometer and Olympus CK2 microscope. Three biological replicate experiments were completed. Data was presented as percent positive for trypan blue compared to a non-stimulated control.

Dichlorofluorescein-diacetate Assay

ROS was measured using fluorescent probe dichlorofluorescein-diacetate (DCF-DA). Culture dishes (35mm) were pre-treated with $2.5 \mu\text{g/ml}$ PEI for 30 minutes before adding 1ml of a 1×10^5 cells/ml HEK cell suspension and incubating for 24 hours at 37°C . Cells were separated into experimental groups consisting of cells pre-incubated

with either 200 units of PEG-catalase for 2 hours, 3mM N-acetyl cysteine for 6 hours, 3mM N-acetyl cysteine for 24 hours, 5 μ M LCS-1 for 24 hours, or 5 μ M VAS2870 for 24h. After pre-incubation, cells were stimulated with 50 μ g/ml *Crotalus atrox* venom for 1, 2, 3 or 4 hours. DCF-DA was added 1 hour before the end of each time point. Cells were subsequently washed 3 times with PBS before adding 1ml DMEM media. DCF-DA fluorescence was measured using an IX71 Olympus microscope with FITC (HQ480 (EX)/Q505LP(BS)/ HQ535(EM)) filters coupled to a Olympus DP71 camera. Phase contrast images (40X) were taken in parallel to fluorescent images. Cellular fluorescence was semi-quantified using ImageJ software (33) by measuring pixel intensity for each cell in digital micrographs. Three biological replicates were completed with 10-30 cells in each image used for quantification.

Statistics

Statistical analysis of AlamarBlue, trypan blue, and DCF-DA assays was carried out using two-tailed t tests in Microsoft Excel software. Data from each assay was represented by two or three biological replicates and normalized against matched non-stimulated controls. Cell viability was calculated as percent of the non-stimulated control and graphed as mean \pm STDV. DCF-DA cellular fluorescence data was graphed as median \pm interquartile range.

Results

Crotalus atrox (CA) induced cytotoxicity

Our initial cytotoxicity studies (not shown) utilized 3-(4,5-dimethylthiazol-2-yl)-5-(3-carboxymethoxyphenyl)-2-(4-sulfophenyl)-2H-tetrazolium (MTS) reagent to monitor cell viability. MTS is a tetrazolium salt that is converted to a soluble form of formazan by

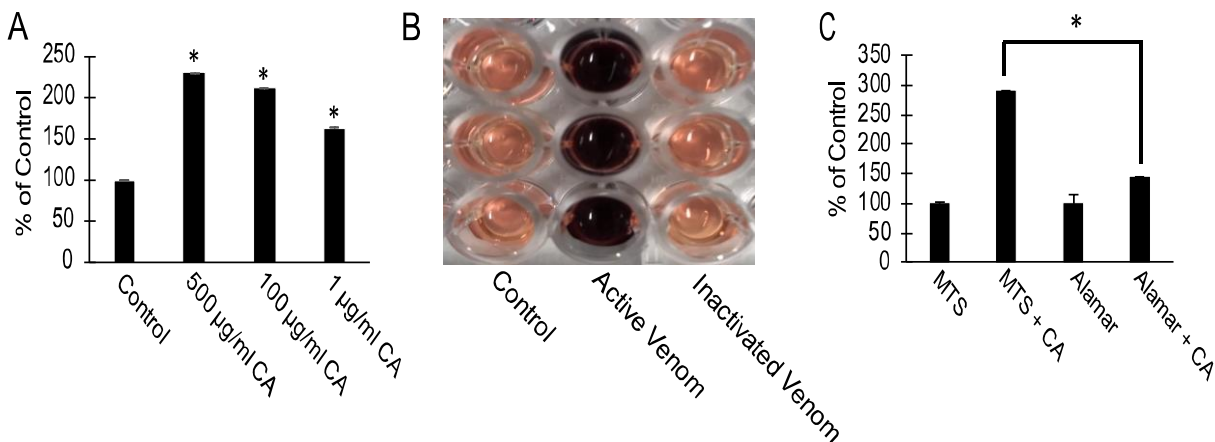


Figure 3. *Crotalus atrox* venom (CA) bioactivity (A) MTS assay. *C. atrox* venom concentrations ranging from 1-500µg/ml were left in DMEM for 10 hours before being exposed to MTS viability reagent. Data is shown as the mean±SD. *P-value<0.05 vs control. (B). Conversion of formazan from MTS caused by 500µg/ml CA venom was compared to that of the same concentration of CA venom that had been heat inactivated. (C) Venom induces more severe changes in MTS than in alamarBlue cell viability reagent. *p<0.05 vs MTS + CA

dehydrogenase enzymes in living cells. To determine if *C. atrox* venom could induce conversion of MTS to formazan without cells present, MTS was incubated with 1, 250, or 500µg/ml venom for 10 hours. Results demonstrated increased venom concentration corresponded to an increase in absorbance (Figure 3A). These findings suggest the bioactivity of the venom converts MTS to formazan. To confirm bioactivity of the venom was responsible for the increased formazan production, 500µg/ml *C. atrox* venom was inactivated by heating at 95°C for 1 minute and compared to untreated venom. Untreated venom reacted with MTS to produce formazan while heat inactivated venom did not produce formazan from MTS. (Figure 3B). The ability of snake venom to convert MTS to formazan can be used as a tool to measure relative bioactivity of *C. atrox* venom. Bioactivity of venom can vary dramatically between lots. This novel method of using MTS to determine venom bioactivity can be used to standardize venom concentrations and bioactivity. As an alternative to MTS, AlamarBlue was tested with and without *C. atrox* venom to insure its accuracy as a cell viability reagent when using

venom as a treatment (**Figure 3C**). AlamarBlue (resazurin) is a cell permeable non-fluorescent blue dye. Upon entering the cell, it accepts electrons from the electron transport chain by acting as a substitute for molecular oxygen. This reduction converts the blue dye into a highly fluorescent pink dye, resorufin (33, 34). Results showed that venom reacted with AlamarBlue, producing resorufin, although the percent of resorufin produced was significantly lower compared to the production of formazan from MTS. *C. atrox* venom (500µg/ml) caused a 2.9-fold increase in formazan production from MTS and only a 1.5-fold increase in resorufin production from resazurin ($p < 0.01$) (**Figure 3C**). Therefore, subsequent experiments utilized AlamarBlue to measure cell viability.

We hypothesized that loss of cellular attachment would lead to cell death during venom stimulation. Therefore, collagen and PEI substrates were tested by growing HEK-293T cells on collagen or PEI then stimulating them with 10, 100 or 500µg/ml *C. atrox* venom for 4 or 10 hours. PEI concentrations of 0.25, 2.5, and 25µg/ml were tested for effects on cell viability during venom stimulation and 2.5µg/ml was selected for its ability to efficiently increase cellular adherence (data not shown). Seeding cells on collagen treated dishes then stimulating with 10, 100, and 500µg/ml *C. atrox* venom for 4 hours resulted in decreased viability values of $93 \pm 9.3\%$, $87 \pm 6.1\%$, and $70 \pm 3.2\%$, which are inversely proportional to venom concentration ($p < 0.05$ vs. non-stimulated control) (**Figure 4A**). Cells seeded on PEI treated dishes then stimulated with 10 or 100µg/ml *C. atrox* venom for 4 hours returned cell viability values of $110 \pm 6.4\%$ and $101 \pm 21.5\%$, respectively, which were not significantly different than non-stimulated controls. However, these values were significantly higher than cells plated on collagen treated dishes suggesting that pre-treating culture dishes with PEI improves cell viability

at lower venom concentrations. Stimulating cells seeded on PEI treated dishes with 500µg/ml *C. atrox* venom for 4 hours significantly decreased cell viability to 66±8.4% compared to the non-stimulated control (p<0.01). There was no significant difference in viability between cells plated on collagen and PEI then stimulated with 500µg/ml *C. atrox* venom for 4 hours (**Figure 4A**).

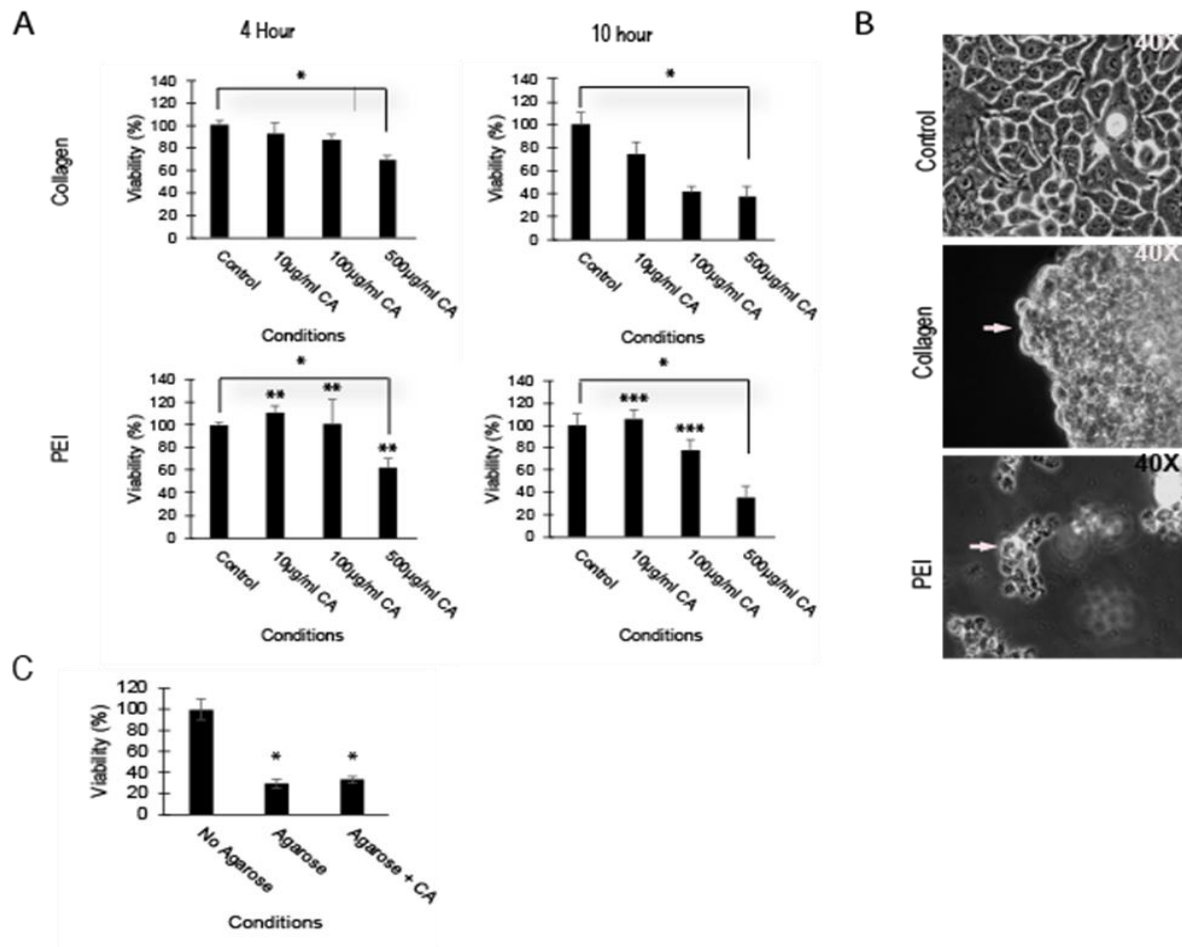


Figure 4. *Crotalus atrox* induced cytotoxicity in HEK cells. HEK cells were grown collagen or PEI treated culture dishes and stimulated with *C.atrox* (CA) venom concentrations ranging from 10-500 µg/ml for 4 or 10 hours. (A) Alamar Blue cell viability assay. Experiments were ran in triplicate with three biological replicates. Data is shown as the mean±SD. *P-value<0.05 vs control. **P-value<0.05 vs Collagen 4 hour. ***P-value<0.05 vs collagen 10 hour. (B) Phase contrast (40X) micrographs we taken of control cells and cells treated with 500 µg/ml CA on collagen or PEI substrates. Arrows in collagen image indicate edge of cellular monolayer. Arrows in PEI images indicate cellular fragments. (C) 96-well plates prepared with and without agarose as a substrate. HEK cells were plated and stimulated with 500 µg/ml CA for 10 hours. Viability was measured using Alamar Blue cell viability assay. Data is show as the mean±SD. *P-value<0.05 vs. nonstimulated control.

To determine if duration of venom stimulation would impede the ability of PEI to improve cell viability, HEK-293T cells were grown on collagen or PEI treated dishes and stimulated with *C. atrox* venom for 10 hours. Cells grown on collagen treated dishes stimulated with 10, 100, or 500µg/ml *C. atrox* venom returned significantly lower cell viability values of 74±9.1%, 41±5.8%, and 37±8.9%, respectively ($p < 0.001$ vs. non-stimulated controls). In contrast, cells grown on PEI treated dishes stimulated with 10 or 100µg/ml *C. atrox* venom returned significantly higher viability values, 106±8.6%, and 78±10.3%, compared to cells seeded on collagen treated dishes ($p < 0.001$). However, stimulating cells seeded on PEI treated dishes with 500µg/ml *C. atrox* venom for 10 hours resulted in a cell viability value of 50±17.1%, which was not significant compared to cells grown on collagen and stimulated with the same conditions (**Figure 4A**).

Phase contrast microscopy was used to examine morphology of cells plated on collagen or PEI substrates, then stimulated with 500µg/ml *C. atrox* venom for 10 hours. Venom stimulation of cells plated on collagen resulted in cells lifting up in a single monolayer while the same treatment of cells plated on PEI resulted in cellular clustering, membrane damage, and lysis as indicated by white arrows (**Figure 4B**).

To better understand if cellular attachment plays a role during venom induced injury, cells were plated on agarose coated dishes and incubated for 24 hours before stimulating with 500µg/ml *C. atrox* venom for 10 hours. Cells plated on agarose alone for 10 hours returned a cell viability value of 29±4.1% ($p < 0.05$ vs control), while cells plated on agarose then stimulated with venom produced a viability value of 32±3.3% ($p < 0.05$ vs control). Results show there was significant loss of viability due to lack of

adherence. However, addition of venom to cells seeded on agarose did not result in increased cell death (**Figure 4C**).

Assessment of membrane integrity

Trypan blue assays were utilized to determine if venom stimulation decreased membrane integrity. Cells were plated on collagen or PEI, then stimulated with 500µg/ml *C. atrox* venom. After 10 hours of stimulation with 500µg/ml *C. atrox* venom, PEI coated dishes demonstrated more cells positive for trypan blue (98±2.2%) than

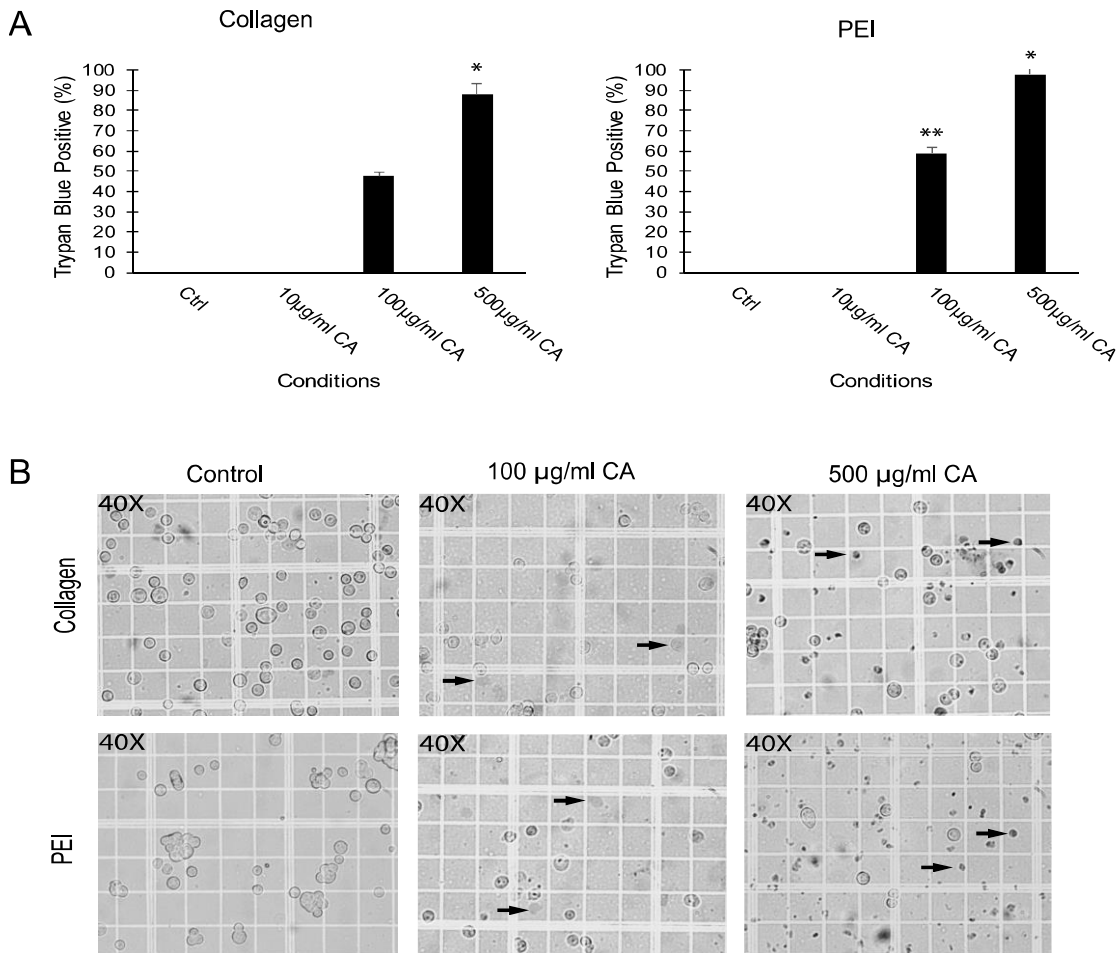


Figure 5. Trypan blue dye exclusion assay. HEK cells were grown on both collagen and PEI treated culture dishes and stimulated with *C. atrox* (CA) venom concentrations ranging from 10-500 µg/ml for 10 hours. Blue cells indicate non-viable. **(A)** Graph of trypan blue positive cells. *P<0.05 vs. control. **p<0.05 vs 100µg/ml CA collagen. **(B)** Brightfield micrographs (40X) were taken of control cells and cells stimulated with 100 µg/ml CA and 500 µg/ml CA on collagen substrate and PEI substrates. Arrows indicate stained cells and cell fragments.

collagen coated dishes ($88\pm 10.9\%$), although this difference was not found to be significant (**Figure 5A**). PEI treated dishes consisted of significantly more trypan blue positive cells ($59\pm 2.9\%$) when stimulated with $100\mu\text{g/ml}$ *C. atrox* venom for 10 hours than collagen treated dishes ($48\pm 2.1\%$) ($p < 0.05$) (**Figure 5A**). Bright field micrographs were taken of cells grown on collagen or PEI and stained with trypan blue after 10 hours of stimulation with 100 and $500\mu\text{g/ml}$ *C. atrox* venom. Cells grown on PEI demonstrated increased fragmentation, membrane damage, and lysis compared to venom stimulated cells plated on collagen, as indicated by arrows (**Figure 5B**).

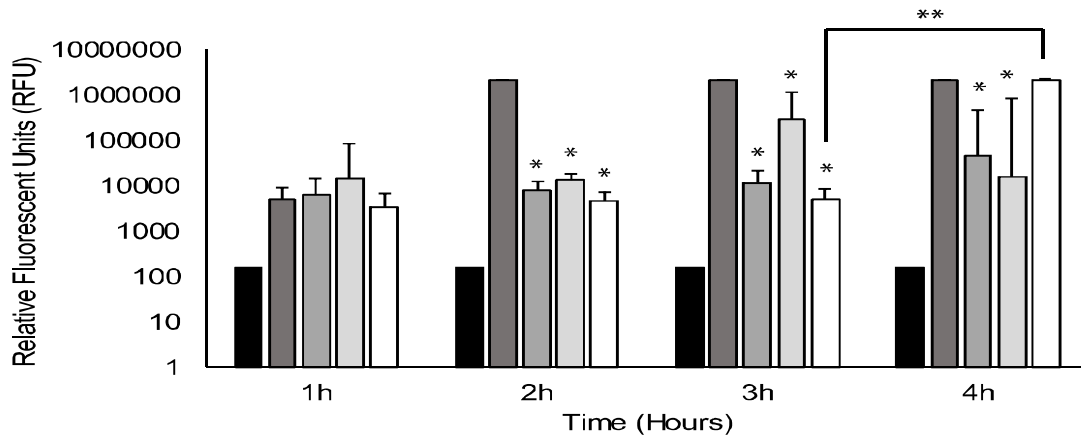
Evaluation of PEG-catalase and N-acetyl cysteine in Crotalus atrox induced ROS production

Dichlorofluorescein-diacetate, an ROS specific fluorescent probe was used to determine if venom stimulation induced ROS production. We utilized a venom concentration of $50\mu\text{g/ml}$ to decrease the rate of cellular detachment. In addition, PEI was used as a substrate to enhance adherence and minimize cell loss during washing steps of DCF-DA assays.

Our results show that HEK cells stimulated for 1 hour with $50\mu\text{g/ml}$ *C. atrox* venom produced RFU values 30-fold higher than non-stimulated cells. Extending the stimulation over a 4 hour time course produced a robust elevation of DCF-DA fluorescence that was 10,000-fold higher in RFU and persisted for 2, 3 and 4 hours of venom stimulation ($p < 0.0001$ vs. non-stimulated control) (**Figure 6**). Pre-treating cells with 200 units PEG-catalase (PC) for 2 hours before stimulating with $50\mu\text{g/ml}$ *C. atrox* venom for 1 hour did not result in significant reduction in DCF-DA fluorescence. However, PEG-catalase pre-treatment significantly reduced DCF-DA fluorescence by

276, 188, and 45-fold after 2, 3, and 4 hours of venom stimulation, respectively (p<0.001 vs. venom alone).

A



B

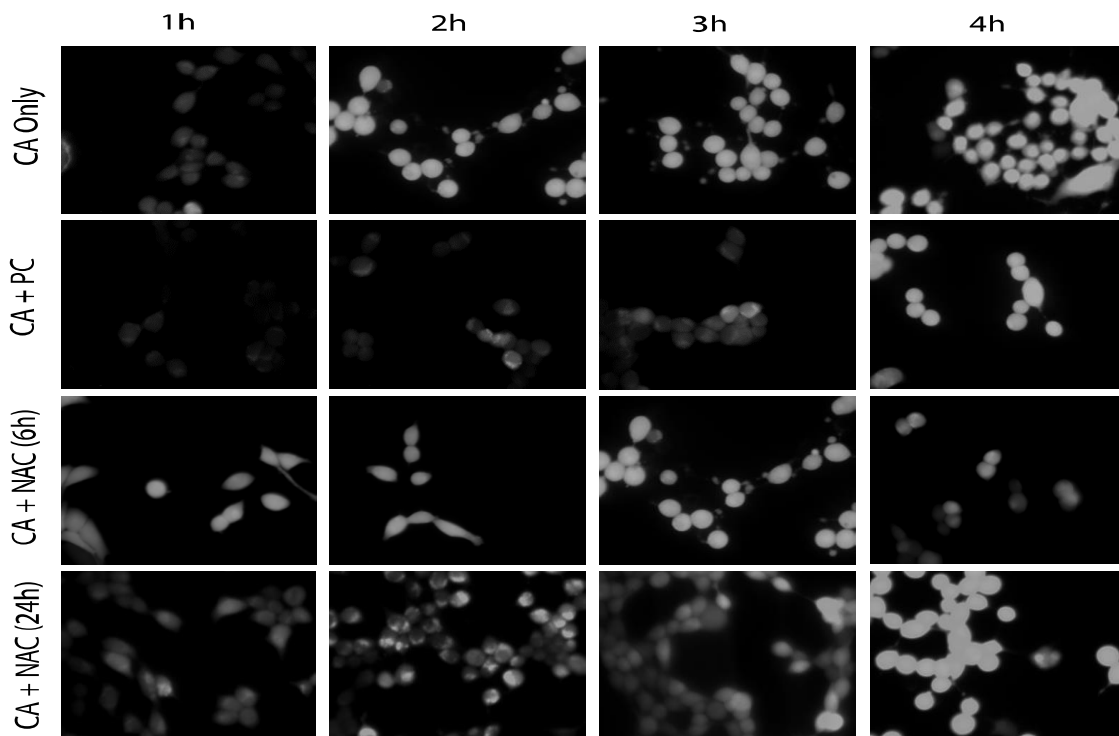


Figure 6. Evaluation of generation of ROS using DCF-DA. **(A)** HEK cells were grown on PEI treated 35mm dishes and separated into treatment groups: Non-stimulated control (■), cells stimulated 50µg/ml *C. atrox* venom alone (CA only ■), cells pre-treated with 200units PEG-catalase before stimulating with 50µg/ml *C. atrox* venom (CA + PC■), cells pre-treated with 3mM N-acetyl cysteine for 6 hours before stimulating with 50µg/ml *C. atrox* venom (CA + NAC-6h■), or cells pre-treated 3mM N-acetyl cysteine for 24 hours before stimulating with 50µg/ml *C. atrox* venom (CA + NAC-24h■). Semi-quantification of ROS-induced fluorescence was complete using imageJ software. *P<0.001 vs. CA only. **P<0.001 compared to CA+NAC(24h) at 3 hours. **(B)** Representative DCF-DA fluorescence images of cells taken over a 4 hour time course taken using an IX71 Olympus microscope coupled to Olympus DP71 camera with FITC filter.

In addition, we used N-acetyl cysteine (NAC) as a non-enzymatic means to control oxidative stress. Cells were pre-treated with N-acetyl cysteine for 6 or 24 hours before stimulating with 50µg/ml *C. atrox* venom. Cells pre-treated with NAC for 6 hours significantly reduced RFU values by 152, 7.3, and 130-fold after 2, 3, and 4 hours of venom stimulation ($p < 0.0001$ vs venom alone). Comparatively, cells pretreated with NAC for 24 hours reduced RFU values by 451, 430, and 1-fold after 2, 3 and 4 hours of venom stimulation ($p < 0.0001$ vs venom alone) (**Figure 6**).

Evaluation of PEG-catalase and N-acetyl cysteine in Crotalus atrox induced cytotoxicity

Our data from figure 6 suggested that ROS are robustly produced after venom stimulation and that pre-incubation with PEG catalase and N-acetyl cysteine reduce the production of ROS in venom stimulated cell. To determine if ROS play a role in *C. atrox* venom-induced cytotoxicity, we followed the same experimental set up as previous cytotoxicity experiments using AlamarBlue to detect changes in cell viability. Cells treated with 200 units PEG-catalase for 2 hours before stimulation with 500µg/ml *C. atrox* venom for 10 hours resulted in $87.4 \pm 5.8\%$ viability compared to $50.0 \pm 17.2\%$ viability of cells stimulated with *C. atrox* venom alone ($p < 0.0001$), representing a 1.5-fold increase in viability for cells pre-treated with PEG-catalase. A similar trend was shown for cells pretreated with NAC for 6 or 24 hours before stimulating with 500µg/ml *C. atrox* venom for 10 hours. Venom stimulated cells pretreated with NAC for 6 or 24 hours resulted in viabilities of $69.1 \pm 9.5\%$ and $81.0 \pm 8.9\%$, respectively ($p < 0.05$) (**Figure 7A**).

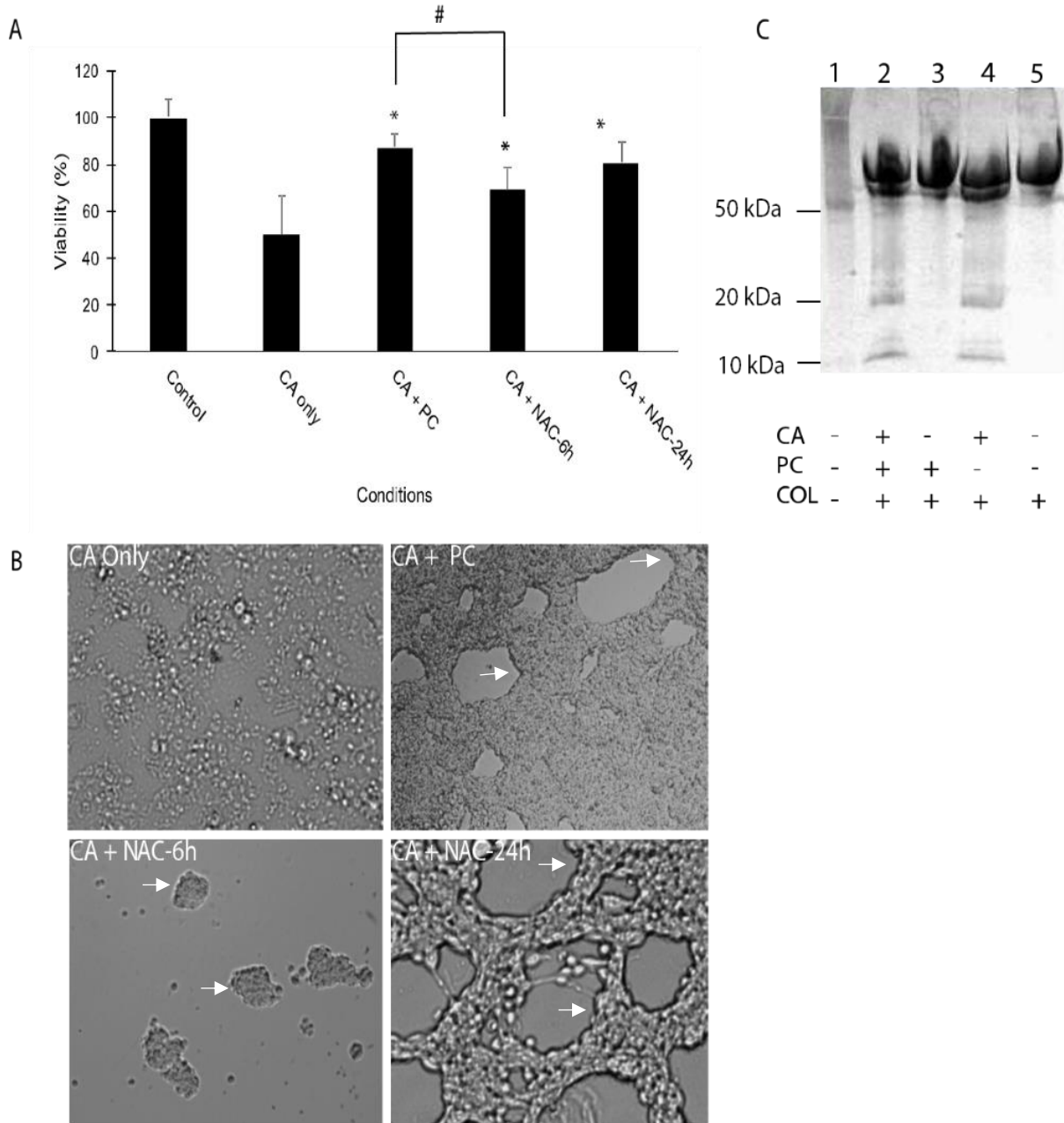


Figure 7. Effects of ROS on cell viability and adherence. **(A)** HEK cells were grown on PEI treated 35mm dishes and separated into treatment groups: cells stimulated 50 μ g/ml *C. atrox* venom alone (CA only), cells pre-treated with 200units PEG-catalase before stimulating with 50 μ g/ml *C. atrox* venom (CA + PC), cells pre-treated with 3mM N-acetyl cysteine for 6 hours before stimulating with 50 μ g/ml *C. atrox* venom (CA + NAC-6h), or cells pre-treated 3mM N-acetyl cysteine for 24 hours before stimulating with 50 μ g/ml *C. atrox* venom (CA + NAC-24h). * $P < 0.05$ when compared to CA only. # $P < 0.05$ when compared to CA+PC. **(B)** Brightfield micrographs of venom stimulated cells pretreated with PEG-catalase or N-acetyl cysteine demonstrate improvements in monolayer integrity and adherence **(C)** SDS-PAGE demonstrates presence of PC does not interfere with ability of venom to enzymatically cleave collagen.

In addition, bright field microscopy was used to evaluate how pretreating cells with PEG-catalase and N-acetyl cysteine influence cellular morphology. Pretreating cells with 200 units PEG-catalase for 2 hours before stimulating with 500µg/ml *C. atrox* venom for 10 hours significantly improves monolayer integrity, as indicated by white arrows (**Figure 7B**, top right) that corresponds with increases in viability that were observed in Figure 7A. As indicated with arrows, cells treated with 3mM N-acetyl cysteine for 6 hours before stimulating with 500µg/ml *C. atrox* venom for 10 hours were lifted but decreased cellular fragmentation was observed when compared to cells treated with venom alone (**Figure 7B**, bottom left). Cells treated with 3mM N-acetyl cysteine for 24 hours before stimulating with 500µg/ml *C. atrox* venom for 10 hours demonstrated improved adherence and decreases in cellular fragmentation similar to PEG-catalase treated cells. (**Figure 7B**, bottom right).

To investigate if PEG-catalase was increasing viability by inhibiting enzymatic components of the venom, we assessed the enzymatic activity of *C. atrox* venom in the absence or presence of PEG-catalase. Collagen is a major substrate for SVMPs and LAAOs present in the venom. Therefore, it can be used to examine the enzymatic activity of *C. atrox* venom. Incubating 1% collagen with 500µg/ml *C. atrox* venom for 10 hours with or without 200 units PEG-catalase produces the same number of cleavage products as seen in lanes 2 and 4 (**Figure 7C**). Our data suggests that enzymatic activity of venom components is not inhibited by the presence of PEG-catalase.

Evaluation of effects of oxidant producing enzymes on generation of ROS and cell viability

To determine if inhibition of key oxidant producing enzymes, NADPH oxidase (NOX) and superoxide dismutase 1 (SOD1), play a role during venom induced cytotoxicity, we used VAS2870 (NOX inhibitor) and LCS-1 (SOD1 inhibitor). Cells were

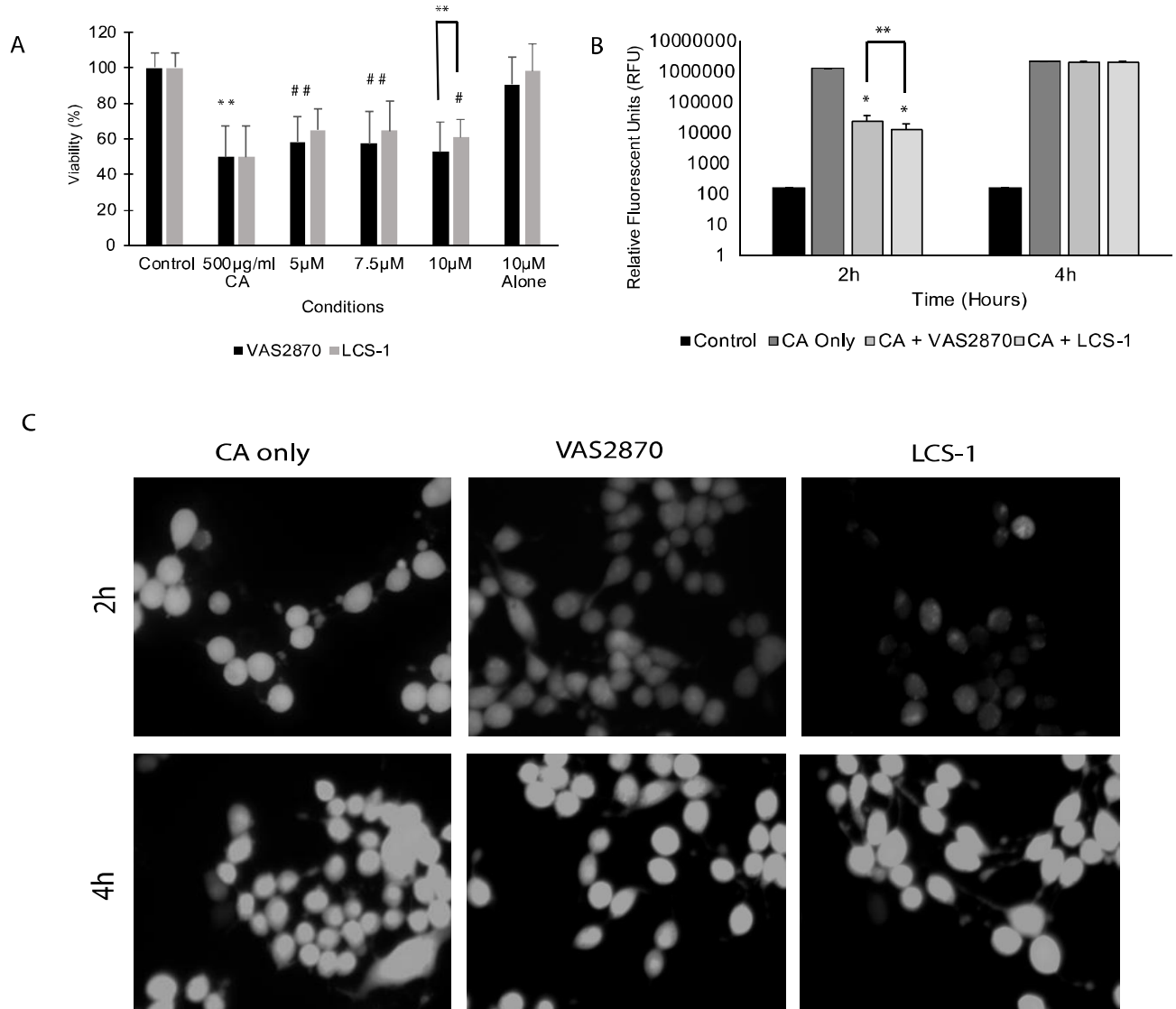


Figure 8. Effects of SOD1 and NOX inhibitors on ROS-induced fluorescence and cell viability. **(A)** AlamarBlue assay. Cells were treated with with 5-10µM VAS2870 or LCS-1 for 24 hours before stimulated with 500µg/ml *C. atrox* venom (CA) for 10 hours. * $P < 0.0001$ compared to control. # $P < 0.05$ when compared to CA only. ** $P < 0.01$. **(B)** DCF-DA assay. Semi-quantification of ROS-induced fluorescence. * $P < 0.01$ compared to CA only. ** $P < 0.05$ compared compared to CA+VAS2870. **(C)** Representative micrographs of HEK cells preincubated with 5µM VAS2870 or 5µM LCS-1 for 24 hours then stimulated with 50µg/ml *C. atrox* venom for 2 or 4 hours.

pre-incubated VAS2870 (5, 7.5 or 10 μ M) and LCS-1 (5, 7.5 or 10 μ M) for 24 hours before stimulating with 500 μ g/ml *C. atrox* venom for 10 hours. Preincubation with 5 μ M VAS2870 resulted in an average of 58.4 \pm 14.2% viability compared to 64.8 \pm 11.6% for cells preincubated with LCS-1. This represents an 8.4% and 14.8% increase in viability compared to cells stimulated with venom alone. Increasing concentration of inhibitors to 10 μ M in negative controls (inhibitor alone) resulting in a cell viability of 90 \pm 15.8% and 98 \pm 15.3% for cells preincubated with VAS2870 and LCS-1, respectively (**Figure 8A**).

To determine if NOX and SOD1 inhibition plays a role in *C. atrox* venom induced ROS generation, HEK293T cells were preincubated with VAS2870 or LCS-1 for 24 hours before stimulating with 50 μ g/ml *C. atrox* venom. DCF-DA was used to monitor intracellular ROS. ROS-induced fluorescence of DCF-DA was measured at 2 and 4 hours. After 2 hours, cells treated with 5 μ M VAS2870 registered a 52 -fold decrease in RFU compared to cells treated with venom alone ($p < 0.0001$). Cells treated with 5 μ M LCS-1 returned a RFU value 100-fold less than cells treated with venom alone ($p < 0.0001$). LCS-1 was significantly more effective at reducing RFU values of cells stimulated with venom for 2 hours than VAS2870 ($p < 0.05$). In contrast, cells pretreated with either inhibitor then stimulated with 50 μ g/ml *C. atrox* venom for 4 hours produced RFU values similar to cells treated with 50 μ g/ml *C. atrox* venom alone for 4 hours (**Figure. 8B**)

Discussion

Edema, local tissue necrosis, and internal hemorrhaging describe early clinical manifestations of *Crotalus atrox* envenomation. If allowed to progress, permanent disfigurement or death can result. The venom destroys tissue at the bite site then enters

the bloodstream, where it inhibits coagulation and activates the surrounding vascular endothelium. Vascular and interstitial tissues respond to venom by initiating an acute inflammatory response leading to vasodilatation, increased permeability, and cell death.

Specific components of *Crotalus atrox* venom, such as SVMs and disintegrins, induce a loss of cellular attachment that can lead to anoikis. SVMs enzymatically cleave type IV collagen while disintegrins physically block integrin interaction with the extracellular matrix. However, other components such as L-amino acid oxidases can directly contribute to ROS concentration levels by producing hydrogen peroxide as by-products of oxidative deamination of L-amino acids (6-10). Therefore, hemorrhagic activity of *C. atrox* venom may induce cytotoxicity indirectly through loss of attachment and directly through the activity of venom components. This is supported by previous work from our lab group that suggests venom stimulation causes increases in ROS and loss of cellular attachment, suggesting that cellular detachment is a critical event during venom induced cytotoxicity (34).

In the first part of this study, different substratum were investigated to determine if adherence improves cell viability during hemorrhagic venom stimulation. Collagen and the polycation polyethylenimine (PEI) were selected. As a native component of the extracellular matrix, collagen allows cells to attach via protein-protein interaction with the integrins on the surface of the plasma membrane while the positive charge of PEI increases the electrostatic interaction with the plasma membrane's negative charge. Considering the ability of the venom to cleave collagen, we predicted that cells grown on PEI would have enhanced adherence resulting in improved cell viability. We chose AlamarBlue to monitor changes in cell viability of cells grown on PEI or collagen then

stimulated with *C. atrox* venom. Our results demonstrated that HEK cells grown on PEI had increased viability when stimulated with lower concentrations (10 and 100µg/ml) when compared to cells grown on collagen. However, higher venom concentrations (500µg/ml) had the same effects on the viability of cells grown on both collagen and PEI (**Figure 4A**). It is reported that coating culture dishes with PEI significantly increases cellular attachment of weakly adherent HEK293T cells compared to culture dishes coated with collagen (35). Pierce et al. (2011) suggests the use of PEI increases the expression of adherence factors, specifically β 1 integrins, in HEK cells (34).

Furthermore, studies by Damiano et al. (1999) show that increasing integrin expression increases survival of cells treated with cytotoxic drugs (36). Increases in adherence induced by PEI may be responsible for improved viability of cells stimulated with 10 and 100µg/ml *C. atrox* venom. Proteolytic activity of higher concentrations of venom (500µg/ml) may be too high for increased adherence to improve viability. This is evident in the clinical presentation of venom injuries where tissue damage at the bite site consists of hemorrhage and tissue damage that progressively decreases with distance.

To better understand cellular detachment as a direct action that contributes to venom cytotoxicity, HEK cells were seeded on dishes coated with agarose to prevent normal cellular attachment. This resulted in significantly reduced cell survival and the addition of venom did not cause further cell death suggesting cell detachment is a part of the cytotoxic response to *C. atrox* venom. This is supported by many studies that have shown that loss of cellular attachment leads to cell death (37-39).

In parallel to cytotoxic studies, we monitored morphological changes occurring in venom stimulated cells. Interestingly, severe cell fragmentation and lysis was observed

in cells plated on PEI when compared to cells plated on collagen, which lifted up in sheets. (**Figure 4B**). Cadherins, proteins that are involved in cell-cell contact, are found within most tissues (40). In collagen treated dishes, the calcium dependent interaction between cadherins may not have been damaged by the activity of the venom allowing cell-cell interactions to remain intact. Furthermore, it is plausible that collagen coated dishes supply SVMPs and LAAOs in *C. atrox* venom with excess substrate not present in PEI coated dishes. Therefore, plasma membrane proteins, such as integrins, G-protein coupled receptors, and ion channels, of cells plated on PEI coated dishes would be more susceptible to enzymatic degradation and potentially increased membrane damage.

Another marker of cytotoxicity is membrane damage, which can be detected by trypan blue. Trypan blue assays revealed that stimulation with 100µg/ml *C. atrox* venom resulted in more trypan blue positive cells in PEI coated dishes compared to collagen coated dishes (**Figure 5**). Higher concentrations of venom (500µg/ml) resulted in comparable amounts of trypan blue positive cells in both collagen and PEI treated dishes. Thus, higher venom concentrations may lead to membrane damage despite the substrate to which cells are bound. AlamarBlue data, in combination with trypan blue data, suggests that stimulation with *C. atrox* venom results in mitochondrial damage and membrane damage that is mitigated by enhancing cellular adherence.

It is reported that noxious stimuli results in cellular retraction and elevated ROS production (34,41). To determine if *C. atrox* venom induces this response in our model, ROS production was monitored during venom stimulation. Our initial experiments showed a robust generation of fluorescence from our ROS probe (DCF-DA), which

reached F_{\max} (Fluorescence Maximum) values after 2 hours of stimulation. Several reports show that pre-incubation with PEG-catalase (PC) or N-acetyl cysteine (NAC) can decrease ROS generated in response to noxious stimuli (10,41-42). For example, Das et al. (2014) demonstrated that NAC significantly reduces ROS levels in cells treated with psoralidin, a compound capable of causing ROS-mediated apoptosis in prostate cancer cells (42). Furthermore, Torii et al. (1997) describes the ability of PC to decrease hydrogen peroxide levels in cells treated with Apoxin I, an L-amino acid oxidase found in *C. atrox* venom (10). Therefore, we utilized PEG-catalase (PC) to enzymatically reduce hydrogen peroxide and N-acetyl cysteine (NAC) to increase the oxidative buffering capacity of cells.

HEK cells pretreated with PC showed a consistent decrease in DCF-DA (RFU) fluorescence (**Figure 6**). Since PEG-catalase specifically catalyzes the conversion of hydrogen peroxide to water, hydrogen peroxide may be a key ROS produced during *C. atrox* venom stimulation. However, under our experimental conditions, DCF-DA fluorescence was not completely abolished suggesting other ROS may be a prevalent part of the intracellular venom response or the production of hydrogen peroxide exceeded the kinetic rate at which exogenously applied PEG-catalase could reduce its formation.

The DCF-DA fluorescence values for cells pretreated with NAC were significantly lower compared to cell stimulated with *C. atrox* venom alone. Cells pretreated with NAC for 24 hours demonstrated a greater reduction in DCF-DA fluorescence compared to cells pretreated for NAC 6 hours. N-acetyl cysteine (NAC), a weak antioxidant on its own, reacts with superoxide and hydrogen peroxide slowly or not at all. However, once

inside the cell NAC is a precursor for glutathione synthesis (43-45). Glutathione (GSH) can directly and non-enzymatically react with free radicals and donate electrons in the reduction of peroxides. Therefore, extended pretreatment (24 hours) may provide more available GSH as a reducing equivalent for GSH peroxidases and the conversion of ROS such as hydrogen peroxide or hydroperoxides to water and molecular oxygen. Interestingly, cells pretreated with NAC for 24 hours showed DCF-DA fluorescence intensity values not significantly different than cells stimulated with venom alone after 4 hours. Overall, this suggests NAC plays an early role (<4hours) in controlling ROS production during venom stimulation.

Next, we examined the effect of PEG-Catalase (PC) and N-acetyl cysteine (NAC) on cytotoxicity using Alamar Blue. AlamarBlue cell viability data suggest that controlling intracellular ROS with PC and NAC in cells stimulated with *C. atrox* venom for 10 hours significantly improves viability. However, venom stimulated cells experienced the greatest improvement in viability when pretreated with PC. Initial experiments with PEG catalase showed no difference in viability when pre-incubated with 100, 200 and 500 units (data not shown). The ability of catalase to improve cell viability in our study is consistent with many other reports (46-49). For example, Venkatesha et al. (2008) suggests that catalase improves viability of human breast epithelial cells stimulated with oxidant-inducing environmental contaminants (49).

Furthermore, greater improvement in viability was observed in venom stimulated cells pretreated with NAC for 24 hours when compared to cells pretreated with NAC for 6 hours (**Figure 7A**), further suggesting that extended duration of NAC pretreatment may allow for enhanced glutathione production. Many studies support the use of NAC

as a method to replenish intracellular glutathione and improve cell viability (50-54). For instance, Soltan-Sharifi et al. (2007) shows that GSH levels are significantly increased in red blood cells after 24 hours of NAC treatment, which matches our experimental time course (53). In addition, Schewiekl et al. (2007) demonstrates the ability of NAC to improve viability by reducing reactive oxygen species in dental pulp cells treated with various dental materials (54).

The protective effect of PC and NAC in venom stimulated cells was further investigated by examining morphology with bright field microscopy. Microscopic inspection revealed cells pretreated with PC demonstrated significant improvements in membrane integrity and lysis compared to cells treated with venom alone. Pretreatment with NAC for 6 hours resulted in decreased cellular fragmentation but loss of attachment was observed. Cells pretreated with NAC for 24 hours demonstrated significant improvements in morphology similar to those pretreated with PC (**Figure 7B**). A study conducted by Song et al. (2010), demonstrates that intracellular reactive oxygen species can interfere with the focal adhesion complex leading to loss of cellular attachment (55). Reducing intracellular reactive oxygen species with PC and NAC may reduce this interference and result in improved cellular attachment and monolayer integrity of venom stimulated cells.

To further expand our study and investigate possible sources of intracellular ROS during venom stimulation, we utilized VAS2870 and LCS-1 to inhibit NADPH oxidases (NOX) or superoxide dismutase 1 (SOD1), respectively. In the cytosol, SOD1 enzymatically converts superoxide to hydrogen peroxide, molecular oxygen, and water (56). NADPH oxidases (NOX) are enzymes present in the plasma membrane that utilize

NADPH to donate electrons to molecular oxygen forming superoxide and hydrogen peroxide (57-69). AlamarBlue assays in combination with inhibitors VAS2870 and LCS-1 were used to elucidate more specific details regarding the production of ROS during venom stimulation. Results demonstrated that both VAS2870 and LCS-1 significantly improve viability of cells stimulated with *C. atrox* venom for 10 hours. LCS-1 resulted in slightly greater cell viability compared to VAS2870 after 10 hours of venom stimulation, although this difference was not found to be significant (**Figure 8A**). We found that pre-incubation with VAS2870 or LCS-1 (concentration range 5.0, 7.5, 10.0 μM) was not as effective at improving cell viability compared to PEG-catalase. This suggests certain hydrogen peroxide producing branches of the oxidative system are not equally involved during venom stimulation. Moreover, VAS2870 is considered a panoramic (pan) inhibitor of NOX isoforms, thus improvement in viability in the presence of VAS2870 may indicate venom stimulation increases the activity of NADPH oxidases. Similarly, cells pre-incubated with LCS-1, showed significant improvement in cell viability suggesting inhibiting SOD1 may lower hydrogen peroxide production.

Inhibition of NOX and SOD1 may be reducing the oxidative response to venom in our experimental model. This is supported by our data that shows that after 2 hours of venom stimulation, cells pretreated with VAS2870 or LCS-1 for 24 hours returned DCF-DA fluorescence (RFU values) 51.9 and 99.6-fold lower than cells stimulated with venom alone. Pretreatment with LCS-1 resulted in venom stimulated cells producing significantly lower RFU values when compared to cells pretreated with VAS2870 (Figure 8B-C). Decreases in DCF-DA fluorescence resulting from the use of LCS-1 or VAS2870 suggests SOD1 and NOX may contribute as sources of intracellular ROS during

envenomation. Since treatment with LCS-1 or VAS2870 did not completely eliminate DF-DA fluorescence, hydrogen peroxide and superoxide may not be the only ROS produced during venom stimulation. Increases in DCF-DA fluorescence seen at 4 hours of venom stimulation in cells pretreated with VAS2870 or LCS-1 suggests other sources of ROS are contributing such as mitochondrial superoxide dismutase (SOD2), xanthine oxidases, and lipoxygenases (60, 61).

Conclusion

Crotalus atrox venom induced cell death correlates with decreases in cellular adherence. At low venom concentrations, cells grown in culture dishes treated with PEI are protected from cell death compared to collagen. However, at equal venom concentrations, increased membrane damage occurs in cells grown on PEI. This suggests the mechanism of cell death may be different depending upon how the cells are anchored. Collagen coated dishes may supply SVMPs and LAAOs present in the venom with excess substrate resulting in cellular detachment (possibly through direct collagen cleavage), while cells grown on PEI lack this substrate likely causing venom enzymes to target the plasma membrane proteins of the cells resulting in decreased membrane integrity.

C. atrox venom stimulation causes robust increases of reactive oxygen species corresponding to decreased viability in HEK-293T. While PEG-catalase, N-acetyl cysteine, LCS-1, and VAS2870 significantly reduce ROS production and improve cell viability, PEG-catalase was the most efficient treatment. Collectively, our data suggests that the mechanism of *C. atrox* venom induced cell death involves several events

including loss of cellular attachment, membrane damage, and a robust production of ROS that could may originate from multiple intracellular sources.

More work is needed to better understand the role of hydrogen peroxide and other ROS during venom stimulation. Current treatment of venomous snakebites involves the use of anti-venom, a systemic application that uses antibodies to neutralize venom components and combat symptoms. However, this treatment does not mitigate local tissue damage and hemorrhage. Elucidating details regarding venom induced local cell death may lead to improved therapeutic treatments for damage at the site of the bite. Further studies could potentially provide new treatment options for injuries caused by venomous snakebites.

Future Directions

Initially, MTS assays were used to measure cell viability. However, cell viability data collected from this assay was inconsistent with cellular morphology of venom stimulated cells. In figure 3, we show that bioactivity of *C. atrox* venom is responsible for the dose-dependent conversion of MTS to formazan when cells are not present. We describe a novel use for MTS as an indicator of venom bioactivity. Throughout this study, MTS reagent was used to normalize *C. atrox* venom to a consistent level of bioactivity that was used in experiments. Future studies in the lab will involve investigating if ROS-producing abilities of L-amino acid oxidases found within the venom effect cellular attachment and ROS levels. Also, a more thorough investigation of possible sources of intracellular ROS during venom stimulation will be conducted involving inhibitors of mitochondrial superoxide dismutase (SOD2), xanthine oxidase, or lipoxygenases. Understanding details of the role of ROS during venom stimulation is

critical for future development of therapeutic treatments for local tissue damages caused by venomous snakebite.

Integration of Thesis Research

Hemorrhagic venom from *C. atrox* is a natural toxin that consists of a mix of bioactive components that function to immobilize and kill prey. Snake venom toxicity and its relation to prey-capture, is an active area of research focused on how foraging behavior may influence venom component concentrations. The main purpose of this study was to investigate *Crotalus atrox* venom induced cytotoxicity. Our data suggests oxidative stress generated through venom stimulation is an important mechanism through which venom immobilizes prey at the cellular level and this information may be applied to the improvement of medical treatment of snakebites.

Acknowledgements

I would like my thesis research advisor Eric Albrecht for the guidance and training necessary to complete all experimental and writing requirements of this educational process. I would like to thank my thesis committee members Thomas McElroy and Carol Chrestensen for their experimental insight and advice. I would like to thank Kennesaw State University MSIB program for the opportunity to work as a teaching assistant for financial assistance.

References

1. Damien Punguyire, Kenneth V. Iserson, Uwe Stolz, Stephen Apanga. Beside Whole-blood clotting times: validity after snakebites. *The Journal of Emergency Medicine*. 2013. 44(3)
2. Calzia, D., Ravera, S., Aluigi, M., Falugi, C., Morelli, A., Panfoli, I. Inactivation of *Crotalus atrox* venom hemorrhagic activity by direct current exposure using Hen's egg assay. *Journal of Biochemical Molecular Toxicology*. 2011. 25:377-381
3. Gutierrez, J., Rucavado, A., Escalante, T., Diaz, C. Hemorrhage induced by snake venom metalloproteinases: biochemical and biophysical mechanisms involved in microvessel damage. *Toxicon*. 2005. 45: 997-1011.:663-667.
4. Pozzi, A., Yurchenco, P., Iozzo, R. The nature and biology of basement membranes. *Matrix Biology*. 2017 57-58:1-11
5. Howes, J., Theakston, R.D.G., Laing, G.D. Neutralization of the haemorrhagic activities of viperine snake venoms and venom metalloproteinases using synthetic peptide inhibitors and chelators. *Toxicon*. 2007. 49: 734-739

6. Takeda, S., Takeya, H., Iwanaga, S. Snake venom metalloproteinases: structure, function and relevance to the mammalian ADAM/ADAMTS family proteins. *Biochimica et Biophysica Acta: Proteins and Proteomics*. 2012. 164-176
7. Andrei, G., Adriana, G., Hajnal, K., Muntean, D. Snake venom metalloproteinases. *Acta Medica Marisiensis*. 2017 62(1): 106-111
8. Shannon, J., Baramova, E., Bjarnason, J., Fox, J. Amino acid sequence of a crotalus atrox venom metalloproteinase which cleaves type IV collagen and gelatin. *The Journal of Biological Chemistry*. 1989. 264(20):11575-11583
9. Du, X., Clemetson, K. Snake venom L-amino acid oxidases. *Toxicon*. 2002. 40: 659-665
10. Izidor, L., Sobrinho, J., Mendez, M., Costa, T., Grabner, A., Rodrigues, V., Silva, S., Zanchi, F., Zuliani, J., Fernandes, C., Calderon, L., Stabeli, R., Soares, A. Snake Venom L-Amino Acid Oxidases: Trends in Pharmacology and Biochemistry. *BioMed Research International*. 2014.
11. Torii, S., Naito, M., Tsuruo, T. Apoxin I, a novel apoptosis-inducing factor with L-amino acid oxidase activity purified from western diamond back rattlesnake venom. *The Journal of Biological Chemistry*. 1997. 272(14): 9539-9542.
12. Galan, J., Snachez, E., Rodriguez-Acosta, A., Soto, J., Bashir, S., McLane, M., Paquette-Straub, C., Perez, J. Inhibition of lung tumor colonization and cell migration with the disintegrin crotatroxin 2 isolated from the venom of *Crotalus atrox*. *Toxicon*. 2008. 51:1186-1196.
13. Huvneers, S., Truong, H., Danen, E. Integrins: Signaling, disease, and therapy. *International Journal of Radiation Biology*. 2007. 83:743-751

14. Giancotti, F., Ruoslahti, E. Integrin Signalling. 1999. *Science*. 285(5430): 1028-1032
15. Santos, A., Corredor, R., Obeso, B., Trakhtenberg, E., Wang, Y., Ponmattam, J., Dvorianchikova, G., Ivanov, D., Shestopalov, V., Goldberg, J., Fini, M., Bajenaru, M. β 1 Integrin-Focal Adhesion Kinase (FAK) Signaling Modulates Retinal Ganglion Cell (RGC) Survival. 2012. *PLoS ONE*. 7(10)
16. Larsen, B., Sorensen, C. The caspase-activated DNase: apoptosis and beyond. *The FEBS Journal*. 2017. 284:1160-1170
17. Fleury, C., Mignotte, B., Vayssiere, J. Mitochondrial reactive oxygen species in cell death signaling. *Biochimie*. 2002. 84:131-141.
18. Ray, P., Huang, B., Tsuji, Y. Reactive oxygen species (ROS) homeostasis and redox regulation in cellular signaling. *Cellular Signaling*. 2012. 24(5):981-990
19. Mailoux, T. Mitochondrial Antioxidants and the Maintenance of Cellular Hydrogen Peroxide Levels. *Oxidative Medicine and Cellular Longevity*. 2018
20. Bolisetty, S., Jaimes, E. Mitochondria and Reactive Oxygen Species: Physiology and Pathophysiology. *International Journal of Molecular Sciences*. 2013. 14(3):6306-6344
21. Halliwell, B. Free radicals, reactive oxygen species and human disease: a critical evaluation with special reference to atherosclerosis. *British Journal of Experimental Pathology*. 1989. 17:737-757.
22. Grau, M., Rigodanza, F., White, A., Soraru, A., Carraro, M., Bonchio, M., Britovsek, G. Ligand tuning of single-site manganese-based catalytic antioxidants with dual superoxide dismutase and catalase activity. *Chemical Communications*. 2014. 50: 4607-4609

23. Bienert, G., Schjoerring, J., Jahn, T. Membrane transport of hydrogen peroxide. *Biochimica et Biophysica Acta* 1758. 2006. 994-1003
24. Young, I., Woodside, J. Antioxidants in health and disease. *Journal of Clinical Pathology*. 2001. 54:176-186
25. Kehrer, J., Klotz, L. Free radicals and related reactive species as mediators of tissue injury and disease: implications for health. *Critical Reviews in Toxicology*. 2015. 45(9): 765-798
26. Bergamini, C., Gambetti, S., Dondi, A., Cervellati, C. Oxygen, reactive oxygen species, and tissue damage. *Current pharmaceutical Design*. 2004. 10:1611-1626
27. Al-Sheikh, Y., Gheneim, H., Aljaser, F., Aboul-Soud, M. Ascorbate ameliorates Echis coloratus venom-induced oxidative stress in human fibroblasts. *Experimental and Therapeutic Medicine*. 2017. 14: 703-713.
28. Khazin, A., Al-Asmari, Riyasdeen, A., Hamed, M., Al-Shahrani, Islam, M. Snake venom causes apoptosis by increasing the reactive oxygen species in colorectal and breast cancer cell lines. *OncoTargets and Therapy*. 2016. 6485-6498.
29. Suzuki, K., Nakamura, M., Hatanaka, Y., Kayanoki, Y., Tatsumi, H., Taniguchi, N. Induction of apoptotic cell death in human endothelial cells treated with snake venom: Implication of intracellular reactive oxygen species and protective effects of glutathione and superoxide dismutases. *Journal of Biochemistry*. 1997. 122: 1260-1264.
30. Zangar, R., Davydov, D., Verma, S. Mechanisms that regulate production of reactive oxygen species by cytochrome p450. *Toxicology and Applied Pharmacology*. 2004. 199: 316-331.

31. Sabharwal, S., Schumacker, P. Mitochondrial ROS in cancer: initiators, amplifiers or an Achilles' heel? *Nature Reviews: Cancer*. 2014. 14: 709-721
32. alamarBlue Cell Viability Assay Technical Manual, DAL 1025, ThermoFisher Scientific.
33. Rasband, W.S., ImageJ, U. S. National Institutes of Health, Bethesda, Maryland, USA, <https://imagej.nih.gov/ij/>, 1997-2018.
34. Pierce, R., Kim, E., Girton, L., McMurry, J., Francis, J., Albrecht, E. Characterization of crude Echis carinatus venom-induced cytotoxicity in HEK 293T cells. *Journal of Venom Research*. 2011. 2:59-67.
35. Vancha, A., Govindaraju, S., Parsa, K., Jasti, M., Gonzalez-Garcia, M., Ballester, R. Use of polyethyleneimine polymer in cell culture as attachment factor and lipofection enhancer. 2004. *BMC Biotechnology*. 4:23
36. Damiano, J., Cress, A., Hazlehurst, L., Shtill, A., Dalton, W. Cell Adhesion Mediated Drug Resistance (CAM-DR): Role of Integrins and Resistance to Apoptosis in Human Myeloma Cell Lines. 1999. *Blood*. 93(5): 1658-1667.
37. McGill, G., Shimamura, A., Bates, R., Savage, R., Fisher, D. Loss of matrix adhesion triggers rapid transformation-selective apoptosis in fibroblasts. 1997. *Journal of Cell Biology*. 138(4): 901
38. Smets, F., Chen, Y., Wang, L., Soriano, H. Loss of cell anchorage triggers apoptosis (anoikis) in primary mouse hepatocytes. 2002. *Molecular Genetics and Metabolism*. 75(4): 344-352.
39. Silginer, M., Weller, M., Ziegler, U., Roth, P. Integrin inhibition promotes atypical anoikis in glioma cells. 2014. *Cell death and disease*. 5:1012

40. Pokutta, S., Weis, W. Structure and mechanism of cadherins and catenins in cell-cell contacts. 2007. *Annual Review of Cell and Developmental Biology*. 23:237-261
41. Kheradmand, F., Werner, E., Tremble, P., Symons, M., Werb, Z. Role of Rac1 and oxygen radicals in collagenase-1 expression induced by cell shape change. *Science*.1998. 280:898–902.
42. Das, T., Suman, S., Damodaran, C. Induction of reactive oxygen species generation inhibits epithelial-mesenchymal transition and promotes growth arrest in prostate cancer cells. 2014. *Molecular Carcinogenesis*. 54:537-547
43. Aruoma, O., Halliwell, B., Hoey, B., Butler, J. The antioxidant action of N-acetylcysteine: its reaction with hydrogen peroxide, hydroxyl radical, superoxide, and hypochlorous acid. *Free Radical Biology and Medicine*. 1989. 6(6): 593-597
44. Rushworth, G., Megson, I. Existing and potential therapeutic uses for N-acetylcysteine: the need for conversion to intracellular glutathione for antioxidant benefits. *Pharmacology and Therapeutics*. 2014. 141(2): 150-159
45. Tobwala, S., Ercal, N. N-acetylcysteine amide (NACA), a novel GSH produg: its metabolism and implications in health. 2013. *Glutathione: Biochemistry, mechanisms of action and biotechnological implications*. Nova Science Publisher. 111-142
46. Arita, Y., Harkness, S., Kazzaz, J., Koo, H., Joseph, A., Melendez, J., Davis, J., Chander, D., Li, Y. Mitochondrial localization of catalase provides optimal protection from H₂O₂-induced cell death in lung epithelial cells. 2006. *American Journal of Physiology*. 290(5): L978-L986.

47. Bai J, Rodriguez AM, Melendez JA, and AIC. Overexpression of catalase in cytosolic or mitochondrial compartment protects HepG2 cells against oxidative injury. 1999. *Journal of Biological Chemistry*. 274: 26217–26224.
48. Dhanasekaran A, Kotamraju S, Kalivendi S, Matsunaga T, Shang T, Keszler A, Joseph J, and Kalyanaraman B. Supplementation of endothelial cells with mitochondria-targeted antioxidants inhibit peroxide induced mitochondrial iron uptake, oxidative damage, and apoptosis. 2004. *Journal of Biological Chemistry*. 279: 37575–37587
49. Venkatesh, V., Venkataraman, S., Sarsour, E., Kalen, A., Buettner, G., Robertson, L., Lehmler, H., Goswami, P. Catalase ameliorates polychlorinated biphenyl-induced cytotoxicity in non-malignant human breast epithelial cells. 2008. *Free Radical Biology and Medicine*. 45(8):1094-1102
50. Rosa, S., Zaretsky, M., Dubs, J., Roederer, M., Anderson, M., Green, A., Mitra, D., Watanabe, N., Nakamura, H., Tjioe, I., Deresinski, S., Moore, W., Ela, S., Parks, D., Herzenberg, L. N-acetylcysteine replenishes glutathione in HIV infection. 2000. *European Journal of Clinical Investigation*. 30(10): 915-929
51. Burgunder, J., Varriale, A., Lauterburg, B. Effect of N-acetylcysteine on plasma cysteine and glutathione following paracetamol administration. 1989. *European Journal of Clinical Pharmacology*. 36(2): 127-131
52. Corcoran, G., Wong, B. Role of glutathione in prevention of acetaminophen-induced hepatotoxicity by N-acetyl-L-cysteine in vivo: Studies with N-acetyl-D-cysteine. 1986. *J Pharmacol Exp Ther* 238: 54–61

53. Soltan-Sharifi, M., Mojtahedzadeh, M., Najafi, A., Khajavi, M., Rouini, M., Moradi, M., Mohammadirad, A., Abdollahi, M. Improvement by N-acetylcysteine of acute respiratory distress syndrome through increasing intracellular glutathione, and extracellular thiol molecules and anti-oxidant power: evidence for underlying toxicological mechanisms. 2007. *Human and Experimental Toxicology*. 26:697-703
54. Shweikl, H., Hartmann, A., Hiller, K., Spagnuolo, G., Bolay, C., Brockhoff, G., Schmalz, G. Inhibition of TEGDMA and HEMA-induced genotoxicity and cell cycle arrest by N-acetylcysteine. 2007. *Dental Materials*. 23(6): 688-695.
55. Song, H., Cha, M., Song, B., Kim, I., Chang, W., Lim, S., Choi, E., Ham, O., Lee, S., Chung, N., Jang, Y., Hwang, K. Reactive Oxygen Species Inhibit Adhesion of Mesenchymal Stem Cells Implanted into Ischemic Myocardium via Interference of Focal Adhesion Complex. 2010. *Stem Cells*. 28(3):555-563.
56. Faraci, F., Didion, S. Vascular protection: Superoxide dismutase isoforms in the vessel wall. *Atherosclerosis, Thrombosis, and Vascular Biology*. 2004. 1367-1373
57. Belarbi, K., Cuvelier, E., Destee, A., Gressier, B., Chartier-Harlin, M. NADPH oxidases in Parkinson's disease: a systematic review. *Molecular Neurodegeneration*. 2017. 12(84).
58. Bedard, K., Krause, K. The NOX Family of ROS-generating NADPH oxidases: physiology and pathophysiology. *Physiological Reviews*. 2007. 87:245-313
59. Shiose, A., Kuroda, J., Tsuruya, K., Hirai, M., Hirakata, H., Naito, S., Hattori, M., Sakaki, Y., Sumimoto, H. A novel superoxide-producing NADPH oxidase in kidney. *Journal of Biological Chemistry*. 2001. 276(2): 1417-1423

60. Cho, K., Seo, J., Kim, J. Bioactive lipxygenase metabolites stimulation of NADPH oxidases and reactive oxygen species. *Molecules and Cells*. 2011. 32(1):1-5
61. Jha, N., Ryu, J., Choi, E., Kaushik, N. Generation and role of reactive oxygen and nitrogen species induced by plasma, lasers, chemical agents, and other systems in dentistry. *Oxidative Medicine and Cellular Longevity*. 2017. 7542540